Structure and properties of protective films of oleic acid formed by immersion and chamber treatment on chemically oxidized magnesium

A.Yu. Luchkin, V.A. Luchkina, I.A. Kuznetsov, O.A. Goncharova, S.S. Vesely and N.N. Andreev

A.N. Frumkin Institute of Physical Chemistry and Electrochemistry, Russian Academy of Sciences, Leninsky pr. 31, 119071 Moscow, Russian Federation
**E-mail: skay54@ya.ru*

Abstract

Applying a conversion coating combined with subsequent application of an inhibitor film is an efficient and popular method to increase the corrosion resistance of metal products. In this work, a set of physical, electrochemical and corrosion methods was used to compare the structure and protective properties of oleic acid films formed on an oxidized surface of Mg90 magnesium from alcoholic solutions and from hot acid vapors. It was shown that both methods resulted in the formation of thin (up to 100 nm) layers on the surface, which increased the protective properties of the oxide coating. The maximum protective effect was shown by the film obtained by one-hour treatment in an alcoholic solution containing 8 mM of the acid. Voltammetric studies showed that this film suppressed anodic dissolution. Using electrochemical impedance spectroscopy, the protective effect was shown to be provided by a mixed blocking–activation mechanism.

Received: October 19, 2023. Published: November 7, 2023 doi: 10.17675/2305-6894-2023-12-4-21

Keywords: *magnesium, corrosion inhibitors, oleic acid, AFM, EIS, oxidation.*

1. Introduction

Magnesium is a promising structural material. However, the low corrosion resistance under atmospheric conditions prevents its wide application [1, 2].

There are many methods for the anticorrosion protection of metals from atmospheric corrosion. The use of inhibitors occupies an important place among these methods. They can be used both independently and in combination with other methods.

Two main types of atmospheric corrosion inhibitors are distinguished, namely, contact and vapor-phase ones:

– contact inhibitors are applied in the form of active substances or solutions directly on the surface to be protected. Preservation by these inhibitors is often performed by immersion (immersion treatment, IT) [3–6].

– vapor-phase inhibitors reach the metal surface as vapors at ambient temperature (volatile inhibitors, VCI) or on heating (chamber inhibitors, CIN).

Inhibitors with high vapor pressure are used as VCIs. It is reasonable to use them if the volume to be protected can be sealed for the entire preservation period. VCIs evaporate at ambient temperature, saturate the volume, reach the metal in the form of vapors, and are adsorbed on it to form protective layers. Many studies deal with the theoretical and practical aspects of their action [7–9]. They can protect both ferrous and non-ferrous metals. However, it has to be stated that there are no efficient volatile corrosion inhibitors for magnesium on the market of temporary metal protection.

The use of CIN is a new approach to vapor-phase protection. Preservation by these compounds (chamber treatment, CT) involves short-term treatment of the metal surface in special chambers with hot vapors of organic compounds that have low volatility at room temperature. In the course of CT, protective adsorption films are formed on the metal, which are stable after the metal is removed from the chamber. This method makes it possible to obtain protective films on metals, including magnesium and its alloys [10].

Some compounds, such as oleic acid (OLA), can be used both as contact inhibitors and as CIN [11]. In such cases, the protection efficiency depends on the technology of inhibitor application and the condition of the metal surface.

In a recent publication [12], we studied the structure and protective properties of surface films formed on air-oxidized magnesium Mg90 from alcoholic solutions and from hot vapors of OLA. It was found that the best protective effect was shown by films obtained by CT. They increase the corrosion resistance of magnesium more than by an order of magnitude.

Chemically oxidized magnesium (OM) is often used in industry. The surface films formed on it upon alkaline treatment have protective effect on their own. However, this effect is not high and development of methods for improving the anti-corrosion properties of OM by chemical oxidation is an urgent task.

Obviously, the presence of a dense oxide film on the metal surface can change the efficiency of inhibitor protection. The purpose of this work, which is a continuation of the previous one [12], was to study the protective properties of oleic acid on OM as a contact and chamber corrosion inhibitor, *i.e.*, upon immersion and chamber treatment.

2. Materials and Procedure

The materials used in this work and the research methods (accelerated corrosion tests at 100% humidity with recurrent condensation of moisture on the samples, atomic force microscopy, ellipsometry, voltammetry, and electrochemical impedance spectroscopy) are similar to those used previously [12]. Prior to the treatment of magnesium samples with the inhibitor, they were oxidized by immersion for 1.5 h in 5 M NaOH solution. The OM was washed with distilled water and air-dried.

To calculate the electrochemical impedance parameters, we used the equivalent circuit (Figure 1) that is widely employed for various metals and alloys [11, 12]:

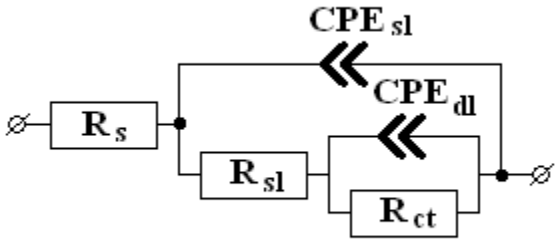

Figure 1. Equivalent circuit used to describe the electrochemical impedance spectra.

In this circuit: R_s is the resistance of the bulk electrolyte between the auxiliary and working electrodes, which does not affect the electrode processes and depends on the conductivity of the medium and on the cell geometry; R_{sl} is the resistance of surface layers (oxide-hydroxide and adsorption ones); R_{ct} is the polarization resistance characterizing the electrochemical kinetics of the corrosion process; CPE_{sl} is the constant phase element characterizing the capacitance of surface oxide and/or adsorption layers; and CPE_{dl} is the constant phase element reflecting the capacitance of the double electric layer. The impedance of the constant phase element was described by the equation:

$$z_{CPE} = A^{-1}(j\omega)^{-n},$$

where A is the proportionality factor; j is the imaginary unit; ω is the complex frequency related to the AC frequency; and n is an exponential factor reflecting the phase deviation, $0 \leq |n| \leq 1$.

Processing of the results and calculation of the equivalent circuit parameters were carried out using the Dummy Circuits Solver program, version 2.1 [10]. The calculated values matched the experimental data within no less than 98%.

The degree of protection of a steel electrode was calculated by the formula:

$$Z = \frac{R^{inh} - R^{bg}}{R^{inh}} \cdot 100\%,$$

where R^{bg} and R^{inh} are the total resistances of the metal-electrolyte interphase interaction including R_{ct} и R_{sl}, before and after electrode treatment, respectively.

The following notation introduced in [12] is also used in this work: τ_{prot} is the time until the first signs of corrosion appear on the samples; i is the current density; E is the potential; E_0 is the starting potential; E_{pit} is the pitting potential; $\Delta E = E_{pit} - E_0$ is the passive area width (anti-pitting basis); and γ is the protection factor.

3. Results and Discussion

3.1. Accelerated corrosion tests at 100% humidity with recurrent condensation of moisture on the specimens

In these tests, we first determined the optimal conditions for the formation of OLA films in the immersion and chamber treatment modes. The key factors are the concentration of the inhibitor in isopropyl alcoholic solution and the treatment time for IT, or the duration and temperature for CT.

OM was significantly superior to uncoated magnesium in terms of corrosion resistance. The time to the appearance of the first corrosion spots on it (τ_{prot}) under the experimental conditions was 20 hours, while it was as small as 0.5 hours on magnesium in the initial state (IS). In both cases, corrosion had the appearance of black dots and spots.

3.1.1. Immersion treatment

Treatment of OM with pure isopropyl alcohol did not affect the corrosion resistance of the metal.

IT in alcoholic solutions of the inhibitor increased the τ_{prot} of oxidized magnesium. In fact, the coating formed in 2 mM solution provided OM protection for 50 hours (Table 1). With an increase in OLA concentration to 8 mM, the protective effect of the surface films increased. Increasing the acid concentration to 16 or 32 mM did not lead to an increase in τ_{prot}. The protective layer formed in 64 mM solution was even less efficient than that obtained in 2 mM solution. At the same time, OLA droplets could be seen with naked eye on the surface of samples treated in alcoholic solutions with concentrations of 16 mM or more. Probably, the decrease in protection is caused by dissolution of protective films in OLA. The corrosion pattern did not change, but it is worthy of note that the first corrosion spots appeared in places where acid droplets were located.

Table 1. Protective effect of adsorption films formed upon OM treatment in OLA solutions with various concentrations. IT duration – 1 hour.

OLA concentration, mM	**0**	**2**	**4**	**8**	**16**	**32**	**64**
τ_{prot}, h	20	50	52	96	96	92	47

Thus, in the case of IT, the 8 mM OLA solution provided the best protective effect.

The results of studies on the effect of IT duration in this solution on the corrosion resistance of the samples are shown in Table 2. The optimum treatment time was 60 min. Shorter treatment led to the formation of films with a poorer protective effect, while increasing the treatment time to 90 minutes or more did not increase the anticorrosion properties of films and was therefore inexpedient.

Table 2. Protective effect of adsorption films formed by OM treatment in OLA solutions for various periods of time. Solution concentration – 8 mM.

IT duration, min	0	5	15	30	60	90	120
τ_{prot}, h	0.5	50	65	82	96	96	96

Thus, IT of oxidized magnesium in 8 mM oleic acid solution provided surface films with the best anti-corrosion properties at a treatment duration of 1 hour.

It should be noted that that the optimal IT conditions for oxidized magnesium (inhibitor concentration – 8 mM, duration 1 h) coincide with the optimal treatment conditions of non-oxidized samples [12].

3.1.2. Chamber treatment

The thermal treatment of OM in air in the *t* range from room temperature to 150°C was not accompanied by an increase in the protective properties of surface films. The first corrosion spots on the samples appeared in 20 hours under the experimental conditions.

Upon CT of samples, the protective effect of adsorption films increased with increasing temperature from room temperature up to 140°C (Table 3). Stronger heating of the chamber was not accompanied by an increase in τ_{prot}. Note that at 140°C a solid matte film was formed on the surface of the samples, which may consist of magnesium oleates and/or OLA polymerization products.

Table 3. Protective effect of adsorption films formed at various temperatures of CT of oxidized magnesium with OLA. Treatment time 1 h.

CT treatment, °C	25	40	60	80	100	120	140	150
τ_{prot}, h	20	24	30	30	35	42	72	72

The data presented in Table 4 show that the maximum efficiency of OM protection is provided by surface films formed in 15 minutes of CT. A further increase of CT time did not change τ_{prot}.

Table 4. Protective effect of adsorption films formed at various durations of CT of oxidized magnesium with OLA. Treatment temperature 140°C.

CT time, min	5	15	30	60	90
τ_{prot}, h	56	72	72	72	72

Thus, the optimal CT conditions for oxidized magnesium are: temperature 140°C, duration 15 minutes. It should be noted that, like in the case of IT, they are the same as the optimum conditions for the treatment of non-oxidized samples [12].

In the case of non-oxidized magnesium, CT provided better protection of the samples [12]. It contrasts, IT better protected chemically oxidized magnesium. Moreover, the corrosion resistance of OM treated under optimal conditions with the inhibitor solution (τ_{prot}=96 h) was smaller than that of the non-oxidized metal after CT also under optimal conditions (τ_{prot}=120 h).

For convenience of discussions on atomic force microscopy, ellipsometry, voltammetry and electrochemical impedance spectroscopy data, let us introduce the designations of various conditions of magnesium treatment (Table 5).

Table 5. Designations of magnesium treatment conditions.

Designation	Treatment conditions
IS	Initial state
A	Oxidized magnesium (background for IT)[1]
B	Oxidized magnesium, treatment for 1 h in 8 mM OLA solution (optimal IT conditions)
C	Oxidized magnesium, thermal treatment for 15 min at 140°C without OLA (background for CT)
D	CT for 15 min at 140°C with OLA (optimal CT conditions)

3.2. Atomic force microscopy

This method makes it possible to study the surface topography. The image of magnesium surface in the initial state shows traces of polishing marks and grains up to 17 nm high (Figure 2 IS). The surface roughness is 7±1 nm.

Chemical oxidation of magnesium resulted in a significant change in the surface topography. Columnar structures presumably consisting of magnesium oxide/hydroxide formed during the oxidation process (Figure 2A). These columnar structures were up to 200 nm large while the average surface roughness increased to 48±13 nm.

OLA adsorption under optimal IT conditions resulted in a cardinal modification of the surface: rounded structures of different sizes formed on it, which completely covered the topography of the substrate (Figure 2 B). The columns characteristic of the oxidized surface were totally hidden under the film that formed. The surface roughness decreased significantly to reach 22±2 nm.

[1] OM treatment with pure isopropyl alcohol did not affect either the corrosion-electrochemical behavior of the metal or the structure of surface films on it. In view of this, treatment conditions A were used in all experiments on magnesium IT described below as the “background” conditions.

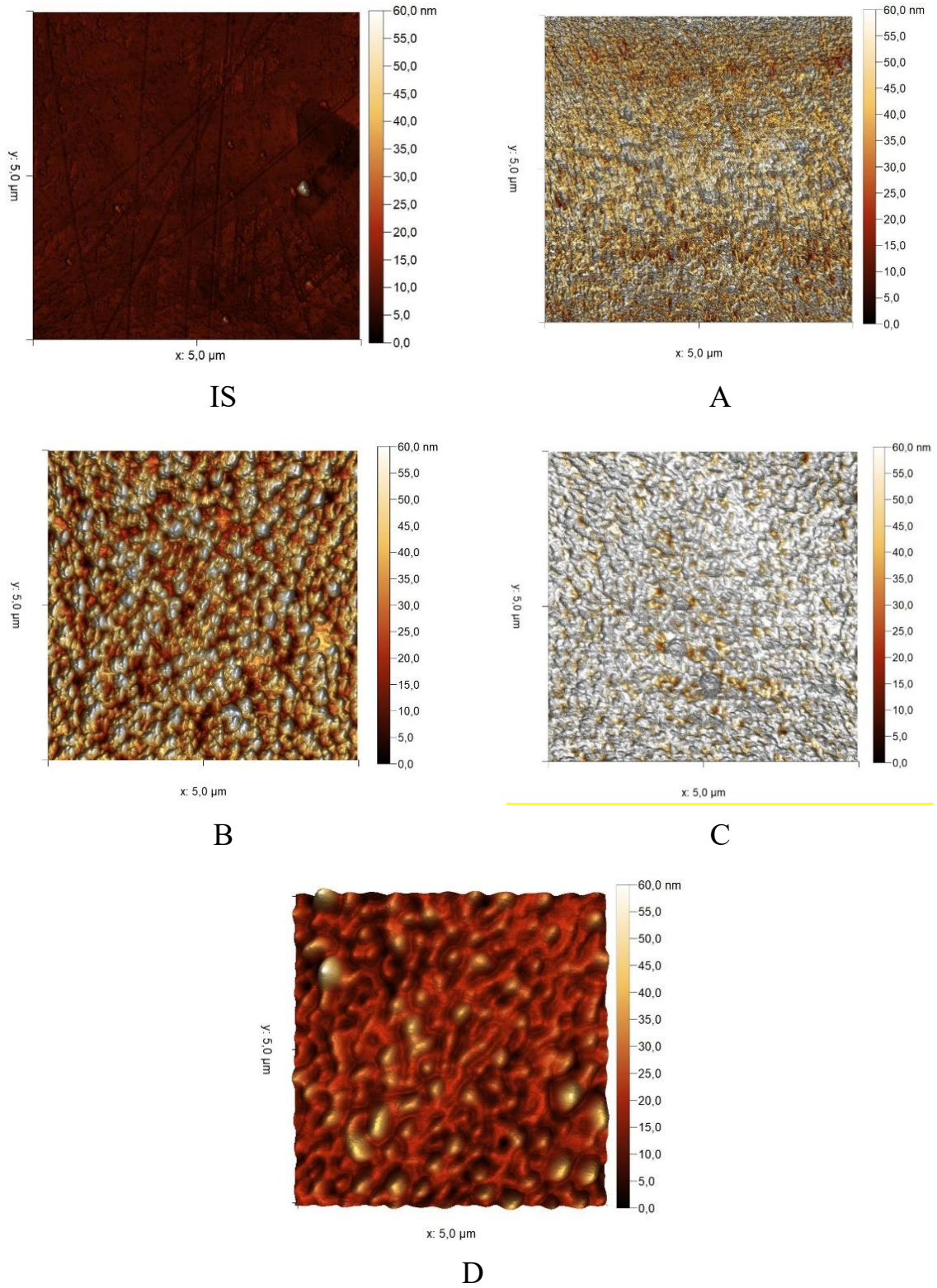

Figure 2. Topography of magnesium surface treated in different modes.

Thermal treatment of the OM surface did not result in any visible changes in the surface topography, as one can clearly see in Figure 1 C. The columnar structures on the sample

surface were almost identical to those on magnesium after oxidation. The surface roughness did not change, either.

CT in the optimal mode led to the formation of various OLA structures on the surface (Figure 2 D) similar to the structures formed by IT under optimal conditions, though under conditions D there are much fewer of them and they are larger. The surface roughness is slightly smaller than after IT and amounts to 16±3 nm. The films formed by CT were visible even to the naked eye.

AFM studies showed that the different deposition methods performed under optimal conditions produced rather thick films differing in structure and completely covering the developed OM surface.

3.3. Ellipsometry

Using the reflective ellipsometry method, the thicknesses of surface layers formed by chemical oxidation of magnesium (treatment A) under optimal IT (B) and CT (D) conditions were estimated. Upon treatment by variant A, an oxide film with a thickness of about 75 nm grows on top of the air-formed oxide. Upon OM inhibitor treatment, its thickness does not change. When samples are treated with OLA, inhibitor films 65 nm thick are formed by IT, and films 100 nm thick are formed by CT on top of the oxide (the latter films are less efficient in corrosion experiments). This fact indicates that the coating thickness is not the factor determining the protective properties in these experiments.

3.4. Voltammetric studies

The results of voltammetric studies are presented in Figure 2 and in Table 6.

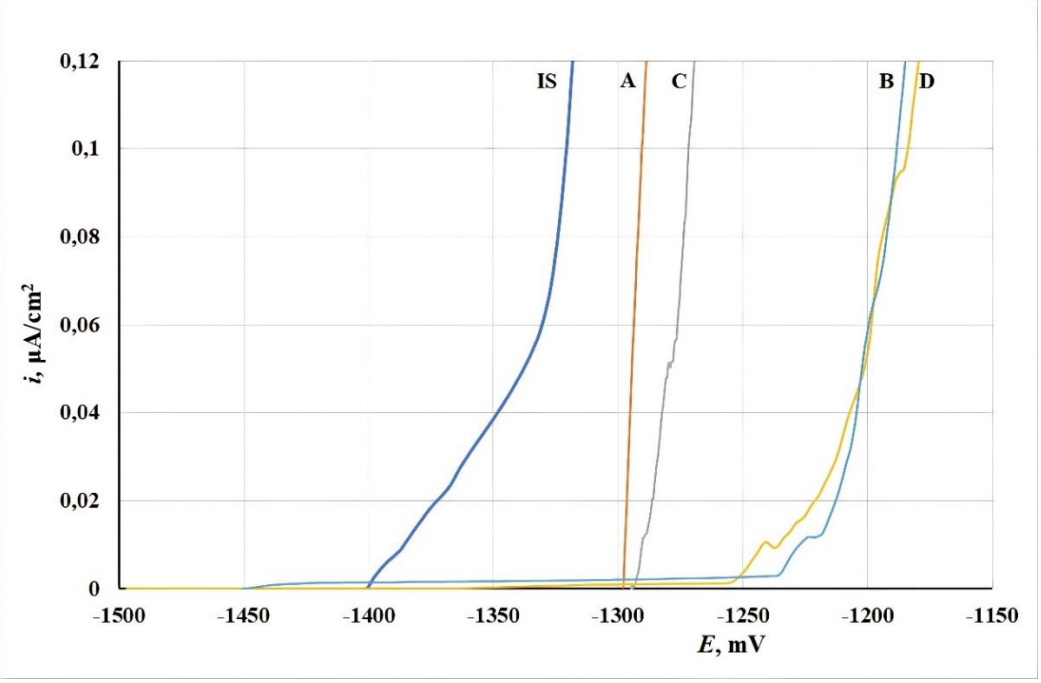

Figure 3. Anodic polarization curves of OM that underwent treatment in various modes.

After immersion of magnesium in the IS into the electrolyte, E_0=−1.40 V was established on it. Upon anodic polarization of the electrode, the current density of metal dissolution increased. There was no metal passivity region on the polarization curves, although their initial region was characterized by a smaller slope of the $i - E$ plots than the region at E >1.33 V. The surfaces of electrodes after their removal from the electrolyte after the polarization experiment were matted.

Magnesium oxidation (curve A) resulted in a noticeable E_0 enrichment (by 0.1 V). At the same time, the shape of polarization plots changed. The region of smooth i growth disappeared. The electrode became, in essence, nonpolarizable, which is characteristic of pitting dissolution of the metal. It can be assumed that pitting occurs in defects of the oxide layer. This is confirmed by inspection of the samples after the experiment. Black dots could be observed on the surface.

Thermal treatment of OM nearly did not change the shape and localization of the curve. The plots A and C were similar in shape and in characteristic values. Their differences were within the data scatter in these experiments.

IT and CT of magnesium under the optimal conditions (curves B and D, respectively) shifted the E_0 values to the cathodic region. At the same time, the polarization curves showed pronounced passive regions more than 0.2 V long, which ended with a sharp i increase due to pitting. Judging by the characteristic values of E, both modes of metal inhibitor treatment are similar in efficiency, though IT is slightly superior to CT. This is consistent with the results of the accelerated corrosion tests described above. It is significant that the protective effect of OLA is associated with the passivation of oxidized magnesium.

Table 6. Characteristics of anodic polarization curves of OM electrodes after surface treatment in various modes.

Treatment	E_0, V	E_{pit}, V	ΔE, V
IS	–1.405	–	–
A	–1.300	–1.300	–
B	–1.450	–1.230	0.220
C	–1.295	–1.295	–
D	–1.495	–1.255	0.240

3.5. Electrochemical impedance spectroscopy

This method makes it possible to obtain additional information about the effect of films on the corrosion process and to determine the mechanism of inhibitor action. The Nyquist plots of the electrodes after treatment in different modes are presented in Figure 4.

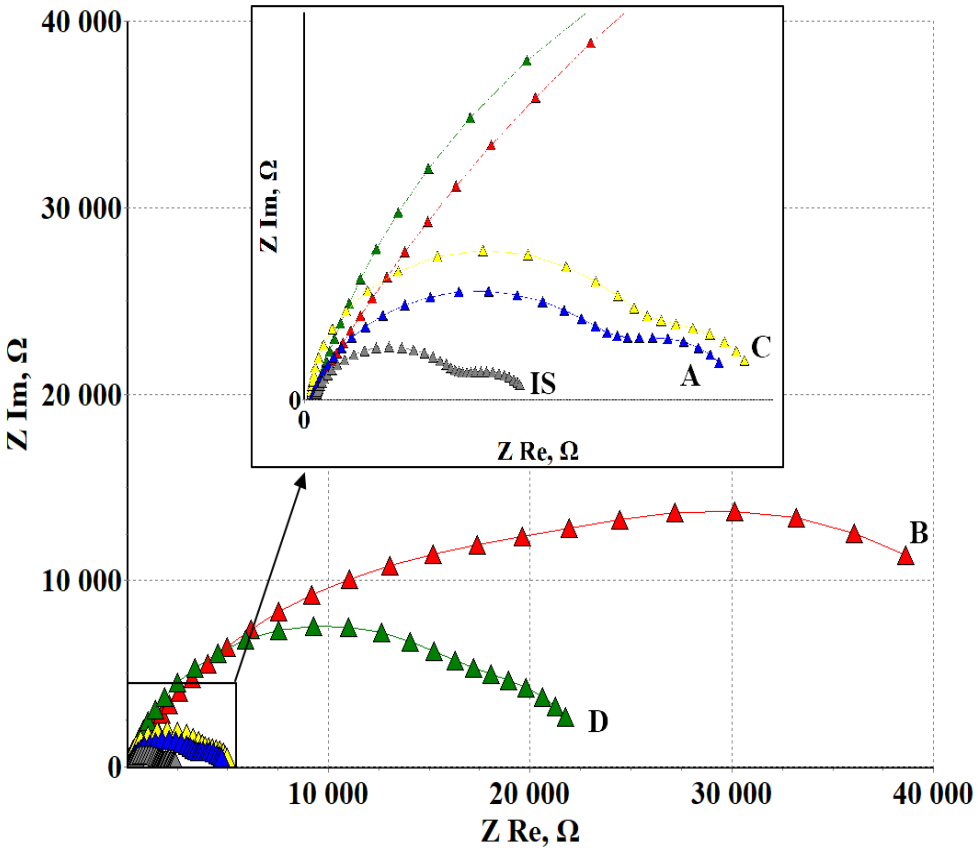

Figure 4. Nyquist plots of magnesium electrodes after treatment in different modes.

The Nyquist plot of a magnesium electrode in the IS has two well distinguishable capacitive loops. According to [11, 12], the first one located in the high and medium frequency region corresponds to the surface oxide–hydroxide layers. The second one with a

smaller radius is localized in the low frequency region. It characterizes the processes occurring in the double layer. According to the results of simulating experimental data by the circuit shown in Figure 1 (Table 7), the main contribution to the charge transfer resistance across the metal–solution interface was made by the surface oxide–hydroxide film: the value of R_{sl} was 2 times larger than R_{ct}. The value of n_{sl} indicates the homogeneity of the oxide–hydroxide film, while the n_{dl} value shows that the electrode processes in the double layer are nearly not complicated by diffusion. The absolute values of CPE_{sl} and CPE_{dl} characterize the initial state of the magnesium surface and serve, along with the values of R_{sl} and R_{ct}, as a starting point for estimating the changes in its properties after metal treatment by various methods.

Magnesium treatment in modes A, B, C, and D did not affect the shape of the hodographs but did affect the values of the elements in the equivalent circuits simulating them.

Chemical oxidation of a magnesium electrode (diagram A) led to a more than twofold increase in the R_{sl} value associated with thickening of the oxide–hydroxide layers (Table 7). At the same time, the value of R_{ct} increased 1.5-fold, apparently due to blocking of a fraction of the surface. The values of CPE_{sl} and CPE_{dl} were close to those for magnesium in the IS.

After chemical oxidation, the magnesium surface became more inhomogeneous. This is also confirmed by the decrease in the value of n_{sl} compared to the IS of magnesium. The n_{dl} value is close to 1, which indicates the absence of inhomogeneous or diffusion-complicated processes in the double layer.

Table 7. Equivalent circuit parameters of OM electrodes treated under various conditions.

	R_r kOhm	CPE_{sl}, $S \cdot s^n$	n_{sl}	R_{sl}, kOhm	CPE_{dl}, $S \cdot s^n$	n_{dl}	R_{ct}, kOhm	Z, %	S, %
IS	0.1	$8.72 \cdot 10^{-6}$	0.88	1.69	$5.9 \cdot 10^{-4}$	0.85	0.75	–	2.21
A	0.1	$1.11 \cdot 10^{-5}$	0.73	3.75	$5.32 \cdot 10^{-4}$	1	1.1	49.51	4.36
B	0.1	$7.77 \cdot 10^{-6}$	0.82	35.21	$4.90 \cdot 10^{-5}$	1	12.71	94.91	1.90
C	0.1	$1.10 \cdot 10^{-5}$	0,76	3.96	$5.06 \cdot 10^{-4}$	1	1.12	52.01	3.51
D	0.1	$4.70 \cdot 10^{-6}$	0.73	18.92	$1.61 \cdot 10^{-4}$	1	3.8	89.27	3.99

IT of magnesium under optimal conditions (variant B) increased R_{sl} and R_{ct} 9- and 12-fold, respectively, relative to OM not treated with the inhibitor (variant A). Relative to magnesium in the IS, R_{sl} and R_{ct} increased by a factor of 20 and 17, respectively. The degree of metal protection calculated from these data reached 94.9%. At the same time, a decrease in the value of CPE_{sl} compared to that of magnesium in state A was observed. According to the value of n_{sl}, IT of electrodes under optimal conditions (B) reduces the inhomogeneity of the surface oxide–inhibitor film. The value of CPE_{dl} indicates an 11-fold decrease in the electrochemically active surface of the metal compared to the OM not treated with OLA (A).

Thermal treatment of OM (treatment mode C) had virtually no effect on the shape of the hodograph and on the calculated values of the elements (comparison of data related to treatment modes A and C).

CT under the optimal conditions (D) resulted in a significant (five-fold) increase in R_{sl} and a less pronounced (three-fold) increase in R_{ct} compared to magnesium treated in mode A. The films formed by CT were heterogeneous; the values of CPE_{sl} and CPE_{dl} changed not too much, namely, *ca*. 2- and 5-fold, respectively. The heterogeneity of the resulting films was shown by the value of n_{sl}. It is noteworthy that the film obtained under optimal CT conditions was significantly inferior in protective properties to the film formed by IT, again under optimal conditions.

The results of simulating the experimental data by the equivalent circuit, like in [12], allow us to numerically estimate the contribution of different mechanisms that provide the inhibitory effect of OLA and to determine the partial corrosion inhibition coefficients.

The values of γ_{bl} and γ_{act} for inhibitor treatment B were calculated using the formulas: $\gamma_{bl}=R_{sl\,B}/R_{sl\,A}$ and $\gamma_{act}=R_{ct\,B}/R_{ct\,A}$, and for treatment D: $\gamma_{bl}=R_{sl\,D}/R_{sl\,C}$ and $\gamma_{act}=R_{ct\,D}/R_{ct\,C}$. The values obtained (Table 8) indicate a mixed blocking–activation mechanism of the inhibitory action of OLA in both (IT and CT) modes for oxidized magnesium treatment.

Table 8. Coefficients of corrosion inhibition by the activation and blocking mechanisms upon OM treatment in various modes.

Treatment conditions	γ_{bl}	γ_{act}
B	9.4	11.55
D	4.78	3.39

4. Conclusions

1. Both immersion and chamber treatment of chemically oxidized magnesium with oleic acid leads to an increase in the corrosion resistance of the metal and inhibition of its anodic dissolution. Immersion treatment is slightly more efficient than chamber treatment.
2. The corrosion resistance of oxidized magnesium treated with oleic acid solution under optimum conditions is lower than that of non-oxidized metal after chamber treatment with oleic acid under optimum conditions.
3. In both variants of magnesium treatment, OLA forms protective films with close thicknesses but different structures on magnesium surface. When the magnesium is dipped in an OLA solution, almost merging rounded agglomerates are formed on magnesium. In the case of CT, the surface films consist of larger structures and are thicker.
4. The protective effect of oleic acid is related to the passivation of chemically oxidized magnesium.
5. Both immersion and chamber corrosion inhibition of oxidized magnesium with oleic acid are characterized by a mixed blocking–activation mechanism.

Financing sources

This study was financially supported by the Russian Science Foundation (Grant no. 23-23-00092 "Development of scientific principles of the self-organization of protective nanoscale films of organic inhibitors on the surface of metals and alloys from the vapor-gas phase").

References

1. T.S.N.S. Narayanan, I.S. Park and M.H. Lee, Strategies to improve the corrosion resistance of microarc oxidation (MAO) coated magnesium alloys for degradable implants: Prospects and challenges, *Prog. Mater. Sci.*, 2014, **60**, 1–71. doi: 10.1016/j.pmatsci.2013.08.002
2. L. Zhao, C. Cui, Q. Wang and S. Bu, Growth characteristics and corrosion resistance of micro-arc oxidation coating on pure magnesium for biomedical applications, *Corros. Sci.*, 2010, **52**, no. 7, 2228–2234. doi: 10.1016/j.corsci.2010.03.008
3. P. Shi, W.F. Ng, M.H. Wong and F.T. Cheng. Improvement of corrosion resistance of pure magnesium in Hanks' solution by microarc oxidation with sol-gel TiO_2 sealing. *J. Alloys Compd.*, 2009, **469**, no. 1–2, 286–292. doi: 10.1016/j.jallcom.2008.01.102
4. J. Liang, B. Guo, J. Tian, H. Liu, J. Zhou, W. Liu and T. Xu, Effects of $NaAlO_2$ on structure and corrosion resistance of microarc oxidation coatings formed on AM60B magnesium alloy in phosphate-KOH electrolyte, *Surf. Coat. Technol.*, 2005, **199**, no. 2–3, 121–126. doi: 10.1016/j.surfcoat.2005.03.020
5. F. Zhu, J. Wang, S. Li and J. Zhang, Preparation and characterization of anodic films on AZ31B Mg alloy formed in the silicate electrolytes with ethylene glycol oligomers as additives, *Appl. Surf. Sci.*, 2012, **258**, no. 22, 8985–8990. doi: 10.1016/j.apsusc.2012.05.135
6. A.A. Chirkunov, A.G. Rakoch, E.V. Monakhova, A.A. Gladkova, Z.V. Khabibullina, V.A. Ogorodnikova, M. Serdechnova, C. Blawert, Yu.I. Kuznetsov and M.L. Zheludkevich, Corrosion protection of magnesium alloy by PEO-coatings containing sodium oleate, *Int. J. Corros. Scale Inhib.*, 2019, **8**, no. 4, 1170–1188. doi: 10.17675/2305-6894-2019-8-4-22
7. K.R. Ansari, A. Singh, A.K. Alanazi and M.A. Quraishi, Chapter 9 – Vapor inhibitors for corrosion protection, in *Eco-Friendly Corrosion Inhibitors*, Ed.: L. Guo, C. Verma and D. Zhang, 2022, 127–136. doi: 10.1016/B978-0-323-91176-4.00012-X
8. Yu.I. Kuznetsov, N.N. Andreev and A.I. Marshakov, Physicochemical Aspects of Metal Corrosion Inhibition, *Russ. J. Phys. Chem. A*, 2020, **94**, 505–515. doi: 10.1134/S0036024420030152
9. F.A. Ansari, C. Verma, Y.S. Siddiqui, E.E. Ebenso and M.A. Quraishi, Volatile corrosion inhibitors for ferrous and non-ferrous metals and alloys: A review, *Int. J. Corros. Scale Inhib.*, 2018, **7**, no. 2, 126–150. doi: 10.17675/2305-6894-2018-7-2-2

10. O.A. Goncharova, A.Yu. Luchkin, I.N. Senchikhin, Yu.B. Makarychev, V.A. Luchkina, O.V. Dement'eva, S.S. Vesely and N.N. Andreev, Structuring of Surface Films Formed on Magnesium in Hot Chlorobenzotriazole Vapors. Materials 2022, **15**, no. 19, 6625. doi: 10.3390/ma15196625
11. O.A. Goncharova, A.Yu. Luchkin, I.A. Archipushkin, N.N. Andreev, Yu.I. Kuznetsov and S.S. Vesely, Vapor-phase protection of steel by inhibitors based on salts of higher carboxylic acids, *Int. J. Corros. Scale Inhib*., 2019, **8**, no. 3, 568–599. doi: 10.17675/2305-6894-2019-8-3-9
12. A.Yu. Luchkin, V.A. Luchkina, I.A. Kuznetsov, A.A. Chirkunov, O.A. Goncharova, Yu.I. Kuznetsov, S.S. Vesely and N.N. Andreev, Structure and properties of protective oleic acid films on magnesium formed upon contact treatment and chamber treatment, *Int. J. Corros. Scale Inhib*., 2023, **12**, no. 4, 1703–1718. doi: 10.17675/2305-6894-2023-12-4-16

♦ ♦ ♦